Tm-Yb-Tm energy transfers and effect of temperature on the fluorescence intensities in oxyfluoride tellurite compounds

Tm–Yb–Tm energy transfers and effect of temperature on the fluorescence intensities in oxyfluoride tellurite compounds

G Özen†‡, J-P Denis, M Genotelle and F Pellé

UPR CNRS 211, Laboratoire de Physico-Chimie des Matériaux, 92190 Meudon, France

Abstract. Up-conversion processes in $PbF_2+TeO_2+WO_3$ glass–ceramics doped with Tm^{3+} and codoped with Tm^{3+} and Yb^{3+} ions were investigated under 680 nm excitation. Emission, excitation and time-resolved spectra and decay profiles were measured at temperatures between 12 and 300 K. A strong blue emission centred at 478 nm originating from the $^1G_4$ level of Tm^{3+} was observed in a doubly doped sample via a two-step energy transfer mechanism, (Tm) $^3F_4 \rightarrow$ (Yb) $^2E_{5/2}$ energy transfer and a positive feedback (Yb) $^2F_{5/2} \rightarrow$ (Tm) $^1G_4$ process, raising the excited Tm^{3+} ion from the $^3F_4$ to the $^1G_4$ level following the absorption of 680 nm excitation light. The time-resolved emission spectra prove the validity of these energy transfer processes.

The optical properties of the excited levels and the energy transfer processes involved in the up-conversion were interpreted using a kinetic model describing the interactions between rare-earth ions in terms of energy migration and luminescence quenching. The microscopic interaction parameter for Tm–Tm intersection in the absence of Yb^{3+} ions was determined to be 6.1×10^{-40} cm^6 s^{-1} in the sample having 1.0 mol% TmF_3. The same parameter for the energy transfer from Tm to Yb was calculated to be 1.2×10^{-38} cm^6 s^{-1} in the sample having 0.15 mol% TmF_3 and 15 mol% YbF_3.

No effect of temperature on the emission intensity of the (Tm) $^3F_4$ level was observed although the emission intensities of the (Tm) $^1G_4$ and (Yb) $^2F_{5/2}$ levels were decreased with increasing temperature. The former decrease accounts for the migration of energy between Yb^{3+} ions and controls the temperature dependence of the blue-up conversion emission.

1. Introduction

There exists an increasing demand for compact visible sources to be used in colour displays, optical recording, biomedical diagnostics and under-water optical communication. In particular, Yb^{3+}-sensitized up-conversion lasers are attractive because of the availability of compact high-power $In_xGa_{1-x}As$ diode lasers to pump the Yb^{3+} absorption band directly [1–3]. Glasses and glass–ceramics are more important hosts than crystals for the up-conversion applications since they can be pumped with a wider range of photons because of their large inhomogeneous widths. A number of promising glass and glass–ceramic hosts have been investigated for producing up-conversion devices. Compounds and compositions involving tellurium dioxide are also used in the production of optical glasses with high refractive indices [4] and other types of glass [5]. Our recent study showed that replacing PbO by PbF_2 increases the blue up-conversion efficiency of infrared light in this matrix [6].

---

† Author to whom correspondence should be addressed.

‡ Present address: Department of Physics, Faculty of Science and Letters, Istanbul Technical University, Maslak, Istanbul, Turkey.

4325

In this work we report the investigation of up-conversion emission upon red excitation. The results reveal a drastic decrease in the intensity of the up-conversion blue emission with increasing temperature although the emission intensity of the $^3F_4$ level stays almost unchanged.

2. Experimental details

The glass–ceramics have been prepared using reagent grade PbF_2, TeO_2, WO_3 and 99.99% purity YbF_3 and TmF_3 as starting materials. The mixtures were melted in a silica crucible with a cover inside an electric furnace at 950 °C. The melt was kept at this temperature for about 30 min and then was poured on a stainless steel plate and pressed with another stainless steel plate.

Powder with grains of approximately the same size (about 5 μm) was made from these samples and fixed homogeneously on a copper plate for fluorescence measurements at low temperatures.

Emission spectra were measured by exciting the samples with light from a DCM dye laser (Coherent 5920) pumped with an Ar^+ laser (Coherent Innova 300) to excite the $^3F_3$ levels of Tm ions. Fluorescence signals were analysed with an HR 1000 Jobin–Yvon monochromator equipped with an RTC 56 TVP photomultiplier in the visible region and a silicon photodiode type PIN-10DP in the IR region. Excitation spectra were recorded in the range 620–700 nm where the ground-state absorption bands of $^3F_2$ and $^3F_3$ levels are located according to the absorption spectrum of Tm^{3+} ions [7]. The intensity of the excitation light was measured with a Coherent 200 power meter at the sample position.

The luminescence decays were measured using a Molectron dye laser with 7 ns duration pumped with a Sopra nitrogen laser (model 2001) as the excitation source. The signal was detected with an RTC 56 TVP photomultiplier tube and then analysed with a PAR 162 boxcar integrator or a Tektronix model 7912AD digitizer interfaced with a PC-AT microcomputer.

For low-temperature measurements, the sample was mounted in a CTI cryostat and the temperature was controlled using a closed-cycle helium refrigerator and an LTS 21-type Lake Shore temperature controller. The sample temperature was varied from 11 to 300 K.

3. Results and discussion

3.1. Spectroscopic properties of the up- and down-conversion emissions

We first investigated the absorption and luminescence properties of the singly doped and codoped samples with Tm^{3+} and/or Yb^{3+} ions. The results were published elsewhere [7]. The absorption spectrum of the codoped sample was found to be the superposition of the absorption spectra of the singly doped samples with Tm^{3+} and Yb^{3+} ions. No measurable effect due to the interaction between Tm^{3+} and Yb^{3+} ions in the doubly doped sample was observed in the absorption spectrum.

The up-conversion emission spectrum of the doubly doped sample in the range 420–530 nm obtained upon 683 nm excitation is shown in figure 1. A strong blue emission centred at 478 nm was observed for a 30 mW cm^{-2} excitation power. This emission corresponds to the $^1G_4 \rightarrow ^3H_6$ transition, and the shape and position of the band correlate well with that obtained by exciting the $^1G_4$ level directly at 458 nm.

The excitation spectrum of this up-conversion emission in the range 630–700 nm is presented in figure 2. The bands observed are centred at 657 and 683 nm and correspond
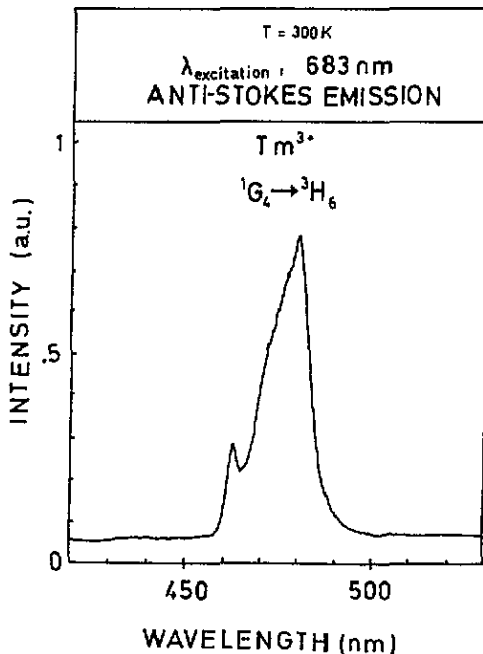
Figure 1. Up-conversion fluorescence spectrum of the sample codoped with 0.15 mol% TmF$_3$ and 15.0 mol% YbF$_3$ upon 683 nm excitation (a.u., arbitrary units).

to the ground-state absorption of the $^3F_2$ and $^3F_3$ levels. Hence these bands have similar features as the absorption bands of Tm^{3+} corresponding to the $^3H_6 \rightarrow ^3F_{2,3}$ transitions.

The emission intensities of the $^1G_4$ and $^3F_4$ levels have quadratic and linear dependences on the excitation power as seen in figure 3. The quadratic dependence of the up-conversion emission indicates that this emission is due to a two-step absorption process. The linear dependence of the $^3F_4$ emission demonstrates that no saturation of this level occurred in the excitation power range of our excitation source.

Figure 4 presents the room-temperature emission spectra corresponding to the (Tm) $^3F_4 \rightarrow ^3H_6$ and (Yb) $^2F_{5/2} \rightarrow ^3F_{7/2}$ transitions followed by the excitation of Tm^{3+} ions into the $^3F_3$ level. Yb^{3+} emission peaking at 965 nm confirms the energy transfer process from Tm^{3+} to Yb^{3+} ions. The excitation spectrum of this emission presents similar features as the absorption bands of Tm^{3+} in the 630–700 nm region which also confirms the energy transfer process.

The time-resolved spectra of the up-conversion emission were measured to understand how the $^1G_4$ level was populated in time. The results are given in figure 5. The luminescence intensity increases in time until about 200 μs, indicating that the up-conversion process is mainly due to an efficient feedback from Yb^{3+} to Tm^{3+} ions via energy transfer processes.

3.2. Dynamics of the (Tm) $^3F_4$ level and Tm–Yb–Tm energy transfer

In addition to the intrinsic decay processes, excited rare-earth ions in an inorganic solid host may relax by firstly different interaction and energy transfer to an acceptor and secondly migration of the excitation until it comes into the vicinity of a quenching centre. In the codoped samples, the fluorescence intensity of each excited level may be affected by the following processes in addition to their intrinsic decay processes:
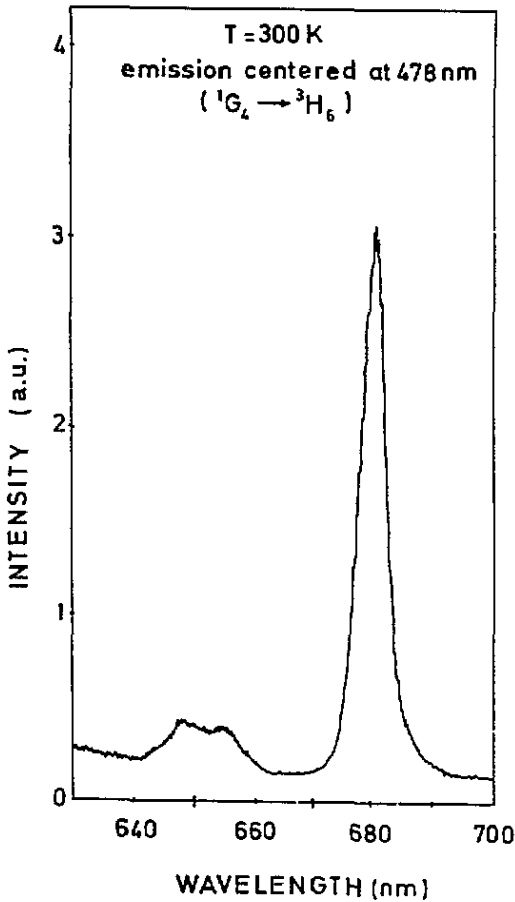
Figure 2. Excitation spectrum of the up-conversion blue emission originating from the $^1G_4$ level of Tm in the sample codoped with 0.15 mol% TmF_3 and 15.0 mol% YbF_3 in the range 630–700 nm (a.u., arbitrary units).

(I) $^3F_4$ level: $^3F_4 \rightarrow {}^2F_{5/2}$ energy transfer;

(II) $^3H_4$ level: intrinsic decay characteristics of the $^3F_4$ level and $^3H_4 \leftrightarrow {}^2F_{5/2}$ energy transfer;

(III) $^3F_{5/2}$ level: $^3F_4 \rightarrow {}^2F_{5/2}$, $^3H_4 \leftrightarrow {}^2F_{5/2}$ and $^2F_{5/2} \rightarrow {}^1G_4$ energy transfer processes, and migration of energy within the Yb^{3+} ions until it is lost to a quenching centre.

The latter process plays an important role in our compounds owing to the high concentration of Yb^{3+} ions (15 mol%). The statistical average of the decay rates corresponding to all these processes contributes to the time dependence of the decay of an excited ion. Hence, the fluorescence lifetime of a metastable level of an excited ion is controlled by the radiative and non-radiative decay processes and is given by

$$1/\tau_f = W_{RD} + W_P + W_E \tag{1}$$

where $W_{RD} = 1/\tau_r$ is the radiative decay rate with τ_r being the radiative lifetime, W_P is the multiphonon relaxation rate and W_E is the energy transfer rate due to the cross-relaxation
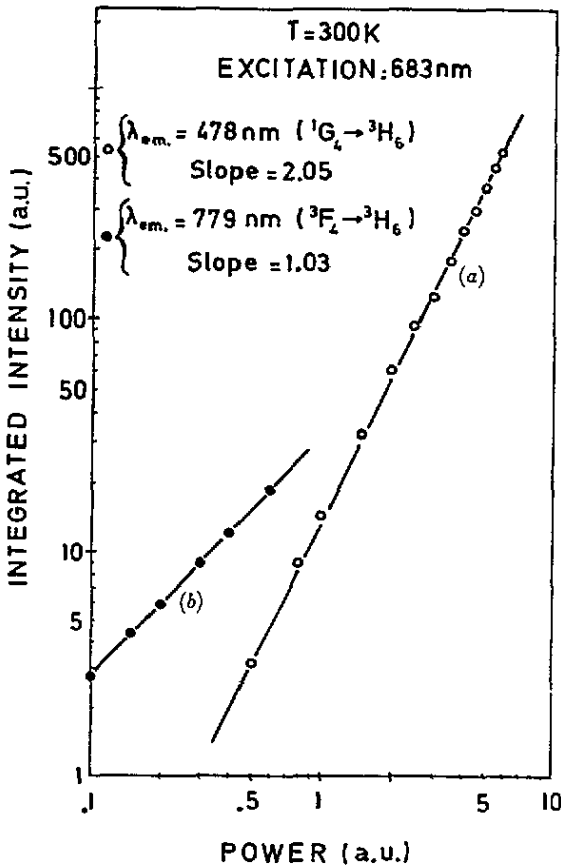
Figure 3. Fluorescence intensities of (a) the $^1G_4 \rightarrow {}^3H_6$ and (b) the $^3F_4 \rightarrow {}^3H_6$ transitions versus the excitation intensity of 683 nm light at room temperature (a.u., arbitrary units).

processes between ions. W_{RD} may be calculated using the theory of Judd [8] and Ofelt [9]. W_P is controlled by the phonon energy of the host and the energy difference to the next lower level. The phonon distribution is given by Planck distribution [10] function $n(T)$ and usually is independent of the active ion concentration.

The fluorescence quantum efficiency of emission from a metastable level can be determined from

$$\tau = \tau_f W_{RD} = \tau_f / \tau_r. \tag{2}$$

The rate of the energy transfer or the cross-relaxation depends on the separation R between the ions. This dependence can be expressed in a multipolar expansion as follows:

$$W_E = C(6)R^6 + C(8)/R^8 + C(10)/R^{10} + \cdots \tag{3}$$

where the first three terms correspond to dipole–dipole, dipole–quadrupole and quadrupole–quadrupole interactions, respectively. If there is a dominant multipolar interaction, then the transfer rate assumes the simpler form

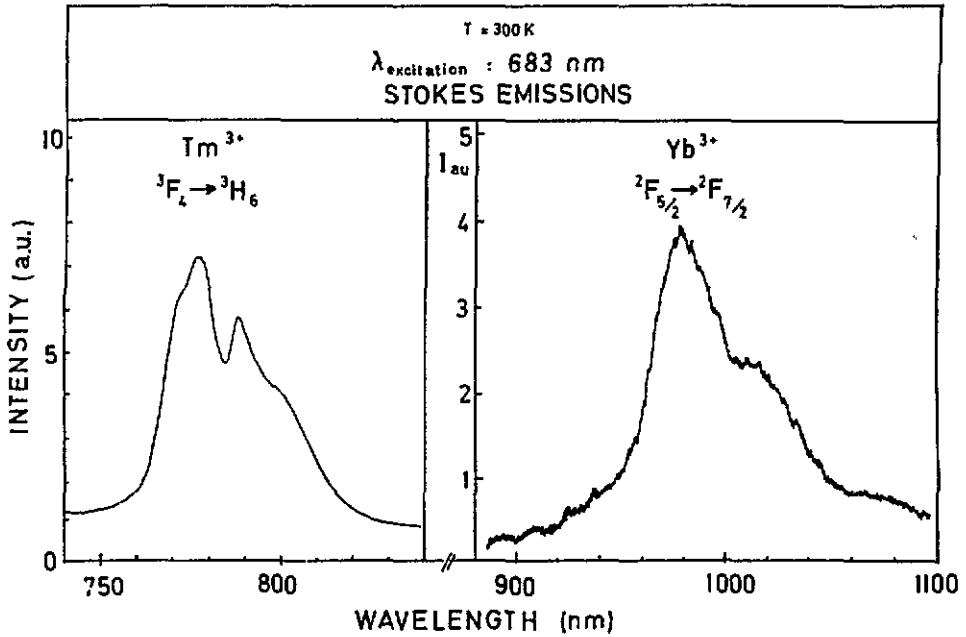$$W_E = \frac{C(n)}{R^n} = \epsilon \tau_0^{-1} \left(\frac{R_0}{R} \right)^n. \tag{4}$$

Figure 4. Spectra of the down-conversion fluorescence from the (Tm) $^3F_4$ and (Yb) $^2F_{5/2}$ levels at room temperature (a.u., arbitrary units).
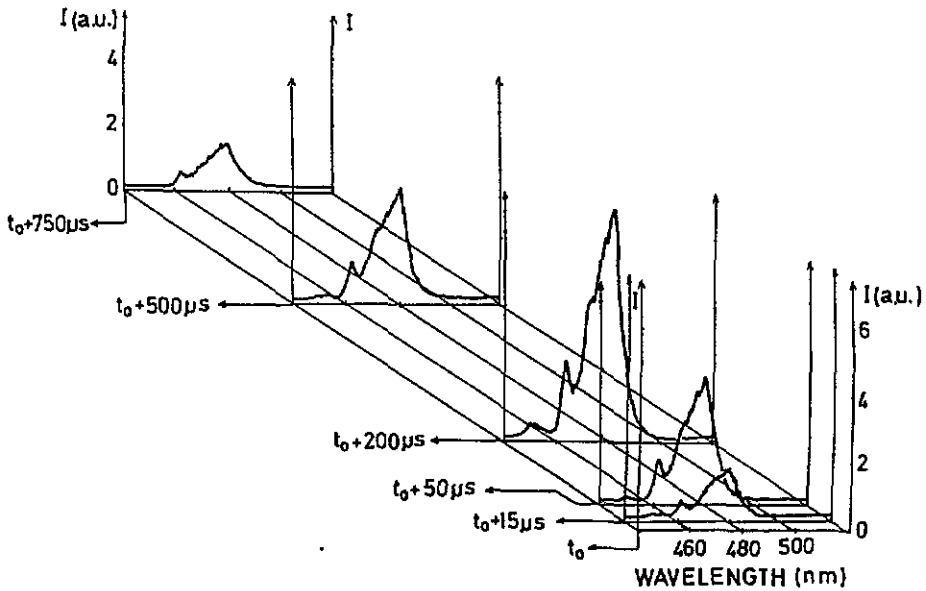

Figure 5. Time-resolved spectra of the up-conversion fluorescence in the sample codoped with 0.15 mol% TmF_3 and 15.0 mol% YbF_3 (a.u., arbitrary units).

In this expression, R_0 is the separation between the ions at which the energy transfer rate

is equal to the decay rate of the donor, and ϵ is the quantum efficiency of the donor luminescence in the absence of interaction between Tm^{3+} ions. The critical interaction distance for this kind of interaction mechanism may then be given by [11, 12]

$$R_0^6 = \frac{3}{4\pi} \left(\frac{hc}{2n\pi} \right)^4 f_A \int \lambda^6 f_{em}(\lambda) f_{abs}(\lambda) \, d\lambda \tag{5}$$

where n is the refractive index of the sample, and $f_{em}(\lambda)$ and $f_{abs}(\lambda)$ are the normalized emission and absorption spectra of the donor and acceptor ions, respectively. f_A is the integrated absorption cross-section of the $^3F_4$ level and is

$$f_A = \frac{mcn}{2\pi^2 e^2 C_A} \int \sigma_A(\omega) \, d\omega \tag{6}$$

where σ_A is the ground-state absorption cross-section of ion A. The parameter $C(n)$ in equation (3) given by $C(n) = R_0^n/\tau_0$ is often called the microscopic interaction parameter and is equal to the probability per unit time of energy transfer when the interacting ions are at the distance of 1.0 cm.
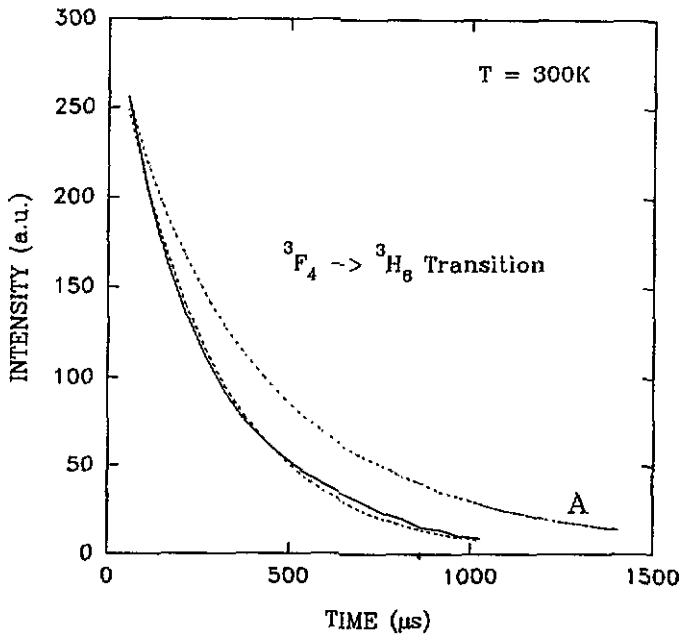

Figure 6. Decay profiles of (Tm) $^3F_4$ fluorescence in glasses single doped with 0.15 mol% TmF$_3$, (A, — · · —) and 1.0 mol% TmF$_3$ (——) upon 683 nm excitation (a.u., arbitrary units) ----, theoretical fit to the latter curve.

The time behaviour of an excited metastable level may be used to examine the cross relaxation and migration-enhanced cross relaxation processes through a theoretical model. The time development of the intensity of the fluorescence, e.g. from the $^3F_4$ level of Tm^{3+}, can be written as [13]

$$I(t) = I(0) \exp[-(A_r t + \gamma t^{1/2} + Wt)] \tag{7}$$

where $I(0)$ is the initial intensity, γ is a parameter describing the cross relaxation without migration and W is the migration-enhanced cross relaxation rate. If the energy migration among the active ions can be ignored, γ has a Förster-like time dependence for the fluorescence decay of a randomly distributed ensemble of ions and is given by $\gamma = \frac{4}{3}\pi^{3/2}\rho_A\sqrt{C_{da}}$, where ρ_A is the acceptor density. When energy migration between the donors occurs, the decay of the donors becomes nearly exponential [14]. In this case, γ becomes equal to $K\rho_A\rho_D\sqrt{C_{da}}\sqrt{C_{dd}}$, where ρ_D corresponds to the density of donors and K is a constant. Then the decay profile of the donor may be analysed using the expression given in equation (7).

In this work we evaluated C_{dd}, the microscopic interaction parameter to characterize the self-quenching of (Tm) $^3F_4$ luminescence, using the decay profile of this emission in the singly doped samples with 0.15 and 1.0 mol% TmF$_3$. The decay profile of this emission in the compound having 0.15 mol% TmF$_3$ content was found to be purely exponential with a lifetime of 433 μs. The decay profile of the same emission was, however, non-exponential at early times after the excitation when the Tm^{3+} concentration was increased to 1.0 mol%. We fit the non-exponential decay to equation (7) by the assumption of the absence of the energy migration between the active ions to obtain the parameter γ, and then to determine C_{dd}, the interaction parameter for the Tm–Tm cross relaxation process. It was determined to be 6.1×10^{-40} cm^6 s^{-1}. The results of the fit and the decay curves of this luminescence are presented in figure 6, and the parameters obtained from the fit are listed together with the decay times measured at room temperature in table 1. We have used the first e-folding time for the decay time of the levels as proposed by Reisfeld and Kalisky [14] if the curve was non-exponential.

Table 1. Concentration dependence of the measured fluorescence lifetimes of (Tm) $^3F_4$ and (Yb) $^2F_{5/2}$ levels, and the efficiencies of forward (Tm) $^3F_4 \rightarrow$ (Yb) $^2F_{5/2}$ and backward (Yb) $^2F_{5/2} \rightarrow$ (Tm) $^1G_4$, $^3H_4$ energy transfer processes at room temperature (C_{Tm} and C_{Yb} denote the TmF$_3$ and YbF$_3$ concentrations, respectively).

C_{Tm}	C_{Yb}	Fluorescence lifetime (μs)		Transfer efficiency $\eta = 1 - \tau_{cd}/\tau_{sd}$	
(mol%)	(mol%)	(Tm) $^3F_4$ level	(Yb) $^2F_{5/2}$ level	(Tm) $^3F_4 \rightarrow$ (Yb) $^2F_{5/2}$	(Yb) $^2F_{5/2} \rightarrow$ (Tm) $^1G_4$, $^3F_4$
0.15	—	433.0	—	—	—
1.0	—	279.0	—	—	—
—	15	—	631.0	—	—
0.15	15	129.0	171.0	0.70	0.73
1.0	15	—	49.0	—	0.92

The efficiency η of Tm–Tm energy transfer via the cross relaxation process may be approximated by the relation $\eta = 1 - \tau_d/\tau_d^0$. The efficiency of this transfer process was calculated to be 0.36 when the Tm content was increased from 0.15 to 1.0 mol% .

Tm–Yb energy transfer was also studied using the same theoretical model for the sample codoped with 0.15 mol% TmF$_3$ and 15 mol% YbF$_3$. The decay curve of the $^3F_4$ luminescence was non-exponential at early times of decay as a result of the Tm–Yb energy transfer process. The decay profile of the Yb emission showing a rise process followed by a decay confirmed that this level was populated via Tm–Yb energy transfer as seen in figure 7. As a result of the transfer, the decay time of (Tm) $^3F_4$ fluorescence became much shorter than it was in the absence of Yb^{3+} ions. We have used the same relation given in equation (7) to determine the interaction parameter C_{da}, since the decay curve of the same emission for 0.15 mol% TmF$_3$ concentration was purely exponential in the absence

of Yb^{3+} ions which indicates the absence of the Tm–Tm cross relaxation processes. The value of 1.2×10^{-38} cm^6 s^{-1} was obtained for the interaction parameter C_{da}. The energy transfer efficiency was also determined and was found to be 0.70.

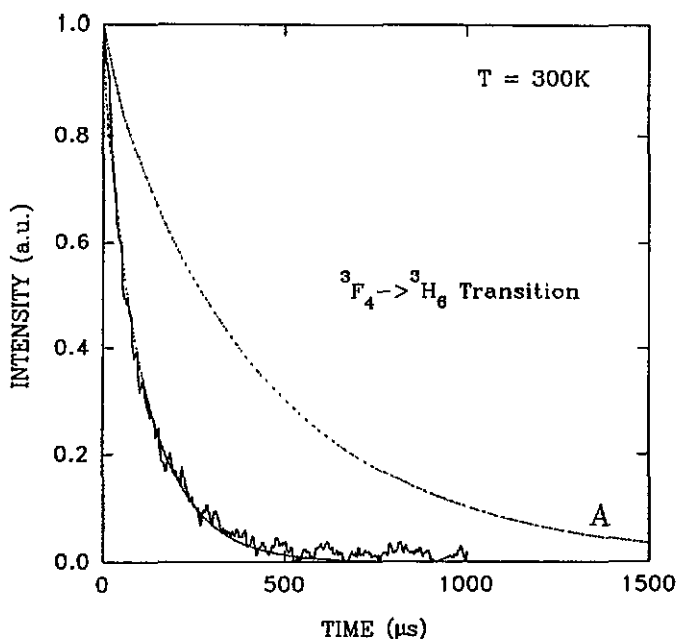**Figure 7.** Effect of Yb^{3+} on the decay profile of (Tm) $^3F_4$ fluorescence in glasses containing 0.15 mol% TmF$_3$, and 0.00 mol% YbF$_3$ (A, — · · —) and 15.0 mol% YbF$_3$ (———), upon 683 nm excitation (a.u., arbitrary units); - - - -, theoretical fit to the latter curve.

Figure 8 presents the effect of Tm on the fluorescence dynamics of Yb^{3+} ions. The effect was studied for two different Tm^{3+} concentrations in the samples having 15 mol% YbF$_3$. Back transfer from Yb to Tm may occur via two different paths: one path is the energy transfer to the $^3H_4$ level of Tm, and the second path is the transfer to the $^1G_4$ level of Tm. The former process results in the up-converted blue emission from the $^1G_4$ level centred at 478 nm. The rise process observed in the time development of the decay profiles of this up-conversion and the Yb^{3+} fluorescence confirm the $^3F_4 \rightarrow {}^2F_{5/2}$ and $^2F_{5/2}^1 \rightarrow G_4$ energy transfer processes as seen in figure 9. The efficiencies of the forward- and back-transfer processes can also be found in table 1.

We also studied the effect of temperature between 12 and 300 K on the excitation energy transfer by measuring the emission intensities of all the excited levels involved in the process. These results are presented in figure 10. To evaluate the temperature dependence of each emission intensity, we need to consider the parameters affecting the optical properties of these levels upon red excitation. The effect of temperature on each emission intensity observed in the codoped sample may be interpreted by considering these processes. According to figure 10, emissions from the (Tm) $^3F_4$ and (Tm) $^3H_4$ and from the (Tm) $^1G_4$ and (Yb) $^2F_{5/2}$ levels show similarities. The emission intensities of the former levels ($^3F_4$ and $^3H_4$) are not affected by the sample temperature. They can both be considered as almost constant between 12 and 300 K. This may be interpreted as an indication of the non-existence of $^2F_{5/2} \rightarrow {}^3F_4$ back transfer. Since the emission intensity
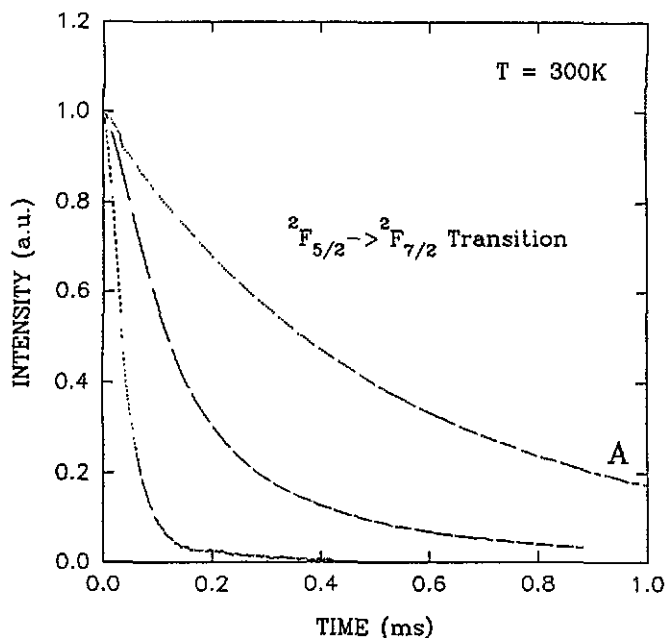
Figure 8. Effect of Tm^{3+} on the decay profile of (Yb) fluorescence in glasses containing 15 mol% YbF_3, and 0.0 mol% TmF_3 (A, — · · —), 0.15 mol% TmF_3 (——) and 1.0 mol% TmF_3 (- - - -), upon 940 nm excitation light from a Ti^+–sapphire laser (a.u., arbitrary units).

of the $^3H_4$ level has a similar temperature behaviour as the emission originating from the $^3F_4$ level, the temperature dependence of this emission is mainly controlled by the intrinsic decay characteristics of the upper level ($^3F_4$). The importance of the intrinsic decay properties of the $^3F_4$ level for the population of the $^3H_4$ level was also confirmed by measuring the relative emission intensities of this level in the presence and absence of the Yb^{3+} ions. The intensity of this emission was found to be much weaker in the presence of Yb^{3+} ions although the up-converted blue emission intensity was much stronger than observed for the singly doped sample with Tm^{3+} ions.

Emissions originating from the $^1G_4$ and $^2F_{5/2}$ levels were affected by temperature in the same manner as seen in figure 10. They both decrease with increasing temperature. This indicates that the temperature dependence of the up-conversion blue emission is mainly controlled by the back transfer and the optical properties of the Yb^{3+} ions in this host. The decrease in the Yb emission intensity with increasing temperature may be explained in terms of the energy migration effect between Yb^{3+} ions which becomes more important at higher temperatures.

4. Conclusion

We have studied the spectroscopic properties of the up-conversion blue emission of Tm^{3+} in $PbF_2 + TeO_2 + WO_3$:Tm^{3+} and/or Yb^{3+} glass–ceramic compounds. Optical parameters such as microscopic interaction parameters were determined for the migration of energy and the energy transfer processes using a kinetic model. The forward- and back-transfer efficiencies were calculated at room temperature and were found to be 0.70 and 0.73 for the
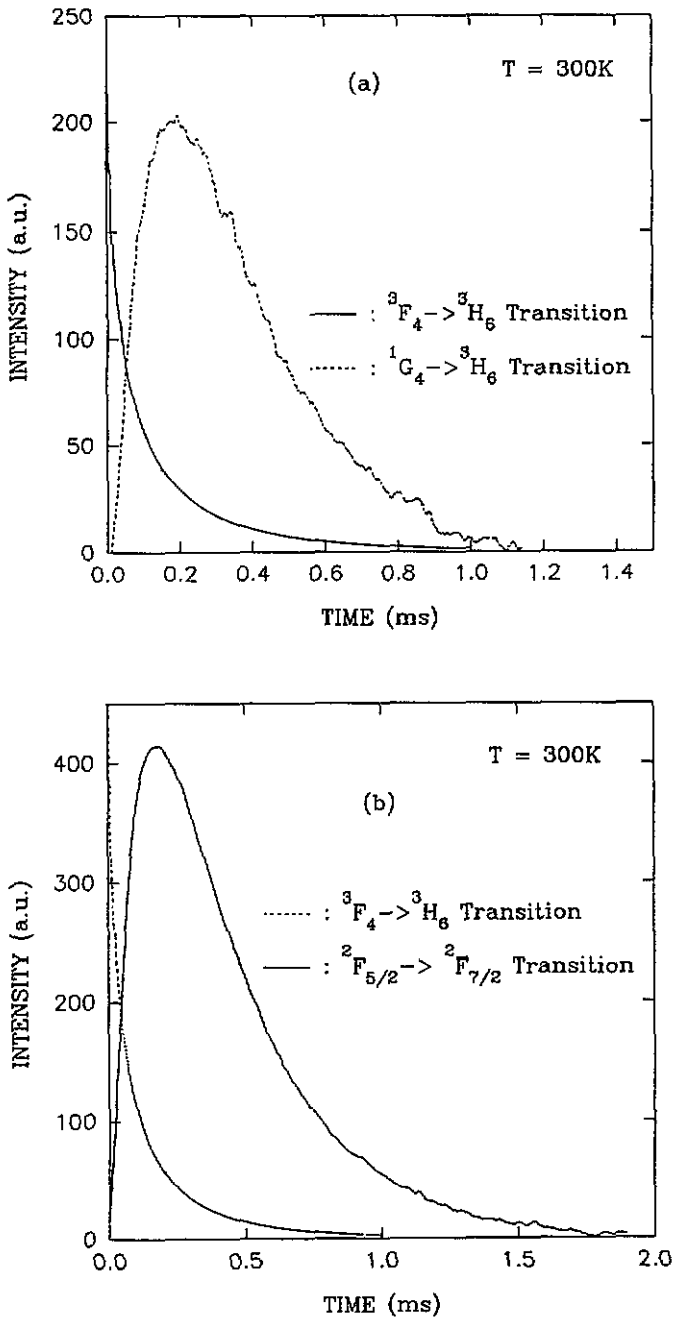
Figure 9. Decay profiles of (*a*) the blue up-conversion fluorescence due to the $^1G_4 \rightarrow ^3H_6$ transition and (*b*) the Yb^{3+} fluorescence as a result of the energy transfer process in glass having 0.15 mol% TmF_3 and 15.0 mol% YbF_3 upon 683 nm excitation (a.u., arbitrary units).

sample doped with 0.15 mol% TmF_3 and 15 mol% YbF_3 while the back-transfer efficiency had the value of 0.92 when the Tm concentration had been increased to 1.0 mol% .

The temperature dependence of up-conversion emission was found to be controlled by
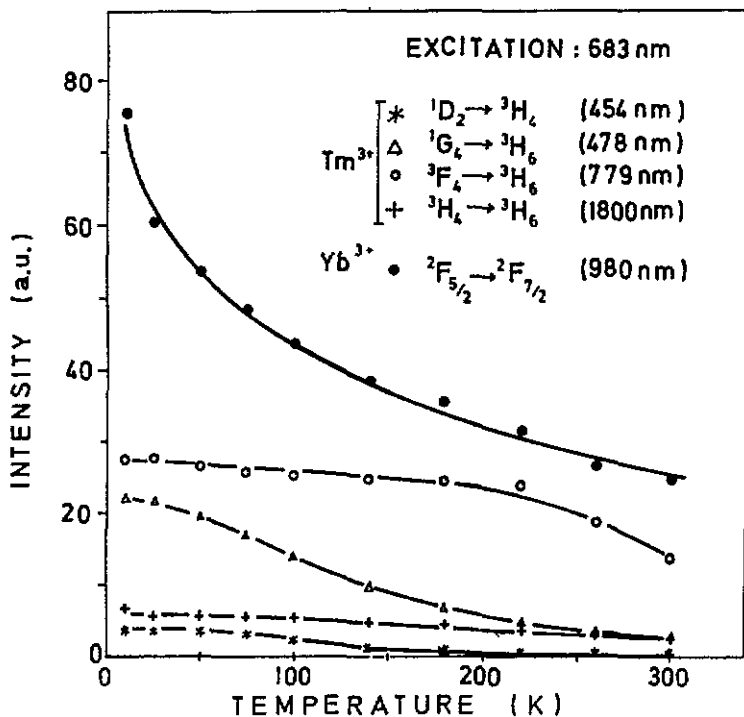
Figure 10. Temperature dependence of all the fluorescence observed in glass codoped with 0.15 mol% TmF$_3$ and 15.0 mol% YbF$_3$ upon 683 nm excitation (a.u., arbitrary units). Lines were drawn to guide the eye.

the temperature dependence of energy migration between the Yb^{3+} ions in these compounds.

References

[1]   Auzel F 1973 *Proc. IEEE* **61** 758
[2]   Auzel F, Pecile P and Morin D 1973 *J. Electrochem. Soc.* **122** 101
[3]   Malta O L, Santa-Cruz P A, de Sà G F and Auzel F 1987 *J. Solid State Chem.* **68** 314
[4]   Zhu Congshan, Lu Xiaojuan and Zhang Zwji 1992 *J. Non-Cryst. Solids* **144** 89
[5]   Heckroodt R O and Res M A 1976 *Phys. Chem. Glasses* **17** 217
[6]   Denis J-P, Kermaoui A, Xu Wu, Özen G and Pellé F 1994 *Eur. J. Solid State Inorg. Chem.* **31** 257
[7]   Denis J-P, Özen G, Xu Wu, Kermaoui A, Pellé F and Blanzat B 1994 *J. Mater. Res.* **9** 1
[8]   Judd B R 1962 *Phys. Rev.* **127** 750
[9]   Ofelt G S 1962 *J. Chem. Phys.* **37** 511
[10] Hirao K, Tamai K, Tanabe S and Soga S 1993 *J. Non-Cryst. Solids* **160** 261
[11] Dexter D L 1953 *J. Chem. Phys.* **21** 836
[12] Inokuti M and Hirayama F 1963 *J. Chem. Phys.* **43** 1978
[13] Ryba-Komanowski W, Golab S, Cichosz L and Jezowska-Trebiatowska B 1988 *J. Non-Cryst. Solids* **105** 295
[14] Reisfeld R and Kaliski Y 1981 *J. Chem. Phys. Lett.* **80** 178